

# ReCalKV: Low-Rank KV Cache Compression via Head Reordering and Offline Calibration

Xianglong Yan<sup>1\*</sup>, Zhiteng Li<sup>1\*</sup>, Tianao Zhang<sup>1</sup>,  
Linghe Kong<sup>1</sup>, Yulun Zhang<sup>1†</sup>, Xiaokang Yang<sup>1</sup>  
<sup>1</sup>Shanghai Jiao Tong University

## Abstract

Large language models (LLMs) have achieved remarkable performance, yet their capability on long-context reasoning is often constrained by the excessive memory required to store the Key-Value (KV) cache. This makes KV cache compression an essential step toward enabling efficient long-context reasoning. Recent methods have explored reducing the hidden dimensions of the KV cache, but many introduce additional computation through projection layers or suffer from significant performance degradation under high compression ratios. To address these challenges, we propose **ReCalKV**, a post-training KV cache compression method that reduces the hidden dimensions of the KV cache. We develop distinct compression strategies for Keys and Values based on their different roles and varying importance in the attention mechanism. For Keys, we propose Head-wise Similarity-aware Reordering (HSR), which clusters similar heads and applies grouped SVD to the key projection matrix, reducing additional computation while preserving accuracy. For Values, we propose Offline Calibration and Matrix Fusion (OCMF) to preserve accuracy without extra computational overhead. Experiments show that **ReCalKV** outperforms existing low-rank compression methods, achieving high compression ratios with minimal performance loss. The code and models will be available at: <https://github.com/XIANGLONGYAN/ReCalKV>.

## 1 Introduction

Large language models (LLMs) [37, 35, 9] have demonstrated outstanding performance across a wide range of tasks. To accelerate inference, modern LLMs cache intermediate Key-Value (KV) states, avoiding redundant computation during autoregressive decoding. However, as the input context length increases, the KV cache grows rapidly, leading to substantial memory overhead and bandwidth pressure. In practice, the KV cache often becomes the primary bottleneck for long-context inference. Consequently, compressing the KV cache is crucial for efficient and scalable deployment of LLMs.

To reduce the size of the KV cache, recent works explore compression along multiple axes. Multi-query attention [33] and grouped-query attention [1] reduce the number of heads by sharing keys and values. Quantization methods [46] lower KV cache’s precision, with some [22, 12] pushing KV representations down to 2 bits. Others [45, 17, 39, 8] reduce the number of cached tokens by selecting only important ones, often based on attention scores. A few methods [4, 21] further compress across layers by reusing KV states. These approaches highlight the multi-dimensional nature of KV cache compression, targeting heads, precision, sequence length, and depth.

Another line of work [5, 20, 19] explores KV cache compression from a different angle—by reducing the dimensionality of the hidden vector space of Keys and Values themselves. For example, MLA [20] reduces memory via low-rank representations but requires training the model from scratch. Other approaches, such as EigenAttention [32] and MastryohakaKV [19], compress KV entries via

\*Equal contribution.

†Corresponding author: yulun100@gmail.com

projection into lower-dimensional subspaces. Although effective, their projection and reconstruction introduce extra decoding overhead, limiting applicability in latency-sensitive scenarios. Palu [5] and LoRC [44] address this issue by directly applying Singular Value Decomposition (SVD) to the KV projection layers, effectively compressing the hidden dimensions of the KV cache. This approach substantially reduces the overhead of runtime projection and reconstruction. However, both methods overlook the inherent asymmetry between Keys and Values in the attention mechanism, and their performance degrades notably under high KV cache compression ratios.

To better explore KV cache compression along the hidden dimension, we conduct detailed analyses of the roles of Keys and Values in the attention mechanism. Our analyses reveal that: **(i)** Most modern LLMs [35, 36, 9] use positional encoding—typically RoPE [34]—which is applied to Keys. As a result, low-rank compressed Keys must be fully reconstructed during inference to enable positional encoding, which introduces additional computational overhead. This makes it essential to consider both accuracy and computational cost when compressing Key cache. **(ii)** We measure the Fisher information of the Key and Value projection layers. Our Fisher information analysis reveals that the Value projection matrices carry significantly higher importance than their Key counterparts, highlighting the crucial role of Value representations in the overall model behavior. Therefore, when compressing the Value cache, it is crucial to minimize accuracy degradation.

Based on our analyses, we develop distinct compression strategies for Keys and Values based on their different roles and varying importance in the attention mechanism. For Keys, we propose **Head-wise Similarity-aware Reordering (HSR)**. It first reorders attention heads based on their representation similarity, then groups similar heads together, and applies grouped SVD within each group. This reduces the Key cache size with low reconstruction overhead. Grouping similar heads helps the SVD better capture shared subspace structures, lowering approximation error and preserving accuracy. For Values, we propose **Offline Calibration and Matrix Fusion (OCMF)**. We first apply SVD to the Value projection matrix, then calibrate the decomposed components using a small calibration dataset. Finally, we fuse the right factor of the SVD decomposition with the subsequent output projection matrix, eliminating the need for explicit reconstruction during inference.

Extensive experiments demonstrate that ReCalKV consistently achieves SOTA performance across multiple LLM families, clearly surpassing existing low-rank compression methods under various evaluation settings. For example, on the LLaMA-2-7B model [36] evaluated on six zero-shot QA datasets, ReCalKV achieves an average accuracy of 63.64% under a 50% KV cache compression ratio, compared to 64.99% for the full-precision model—corresponding to only a 2% relative drop. Notably, since ReCalKV is orthogonal to quantization techniques, it can be seamlessly integrated with them to achieve even higher overall compression ratios.

Our key contributions can be summarized as follows:

- We propose ReCalKV, a novel post-training KV cache compression framework that reduces memory overhead in long-context inference without requiring model retraining.
- We propose the Head-wise Similarity-aware Reordering (HSR) strategy for Key compression, which effectively reduces the Key cache size with limited reconstruction overhead.
- We propose the Offline Calibration and Matrix Fusion (OCMF) strategy for Value compression, preserving accuracy without added computation.
- Extensive experiments demonstrate that ReCalKV consistently outperforms prior low-rank compression approaches. Furthermore, ReCalKV can be seamlessly combined with quantization techniques to achieve even higher compression ratios.

## 2 Related work

**SVD-Based LLM Compression.** Singular Value Decomposition (SVD) has been widely adopted for compressing LLMs by approximating weight matrices with low-rank factors. However, standard SVD [25] has been observed to cause notable performance degradation in practice. To address this, FWSVD[13] incorporates Fisher information to guide decomposition, while ASVD[40] rescales weights to mitigate the impact of activation outliers. SVD-LLM[38] establishes a direct connection between singular values and compression loss, employing data whitening and selective truncation to minimize degradation. AdaSVD[18] further improves compression by introducing adaptive rank allocation and compensation mechanisms. Unlike prior methods that target model weights, we apply SVD to the key and value projections to compress the KV cache directly.

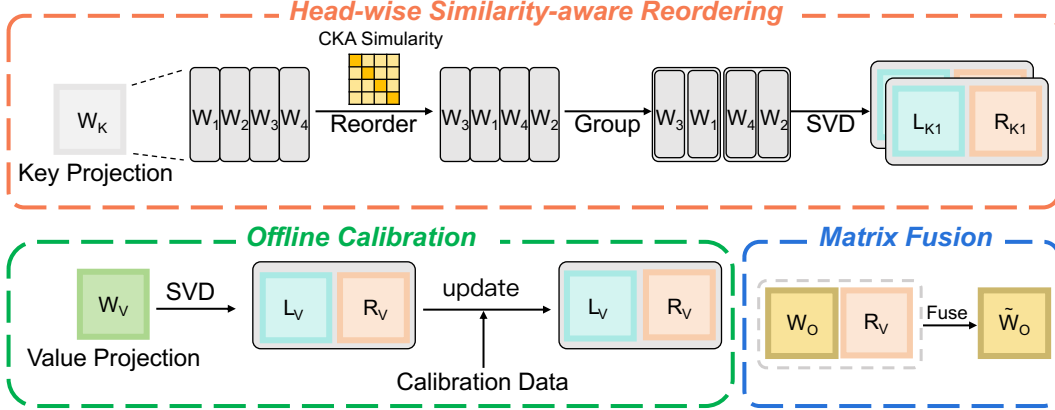


Figure 1: **Overview of the ReCalKV framework.** The method consists of three key components: Head-wise Similarity-aware Reordering (HSR) for compressing Keys via grouped SVD, and Offline Calibration and Matrix Fusion (OCMF) for compressing Values without additional runtime overhead.

**KV Cache Compression.** To support long-context inference, various methods have been proposed to compress the KV cache. Quantization-based approaches are widely adopted: Atom[46] performs per-token quantization, while WKVQuant[41] uses a two-level scheme for better accuracy. KIVI[22] and KVQuant[12] combine per-token and per-channel quantization, with KVQuant further leveraging non-uniform and sparse techniques to handle outliers. In parallel, token eviction methods [45, 17, 39, 8] reduce memory by discarding less relevant tokens or retrieving only subsets during decoding. Beyond these strategies, several methods aim to reduce the hidden dimension of KV representations. DeepSeekV2[20] uses MLA for built-in dimension reduction, but requires training from scratch. MatryoshkaKV[19] and Eigen-Attention[32] project the KV cache into a low-rank space via additional projection matrices, at the cost of increased computation. HeadKV [10] uses SVD to reduce the number of KV heads, leading to improved efficiency. LoRC[44] and Palu[5] directly apply SVD to the KV projection matrices, reducing dimensionality with minimal architectural changes. Our method is a post-training low-rank KV compression approach and is orthogonal to quantization and token eviction, enabling easy integration for further compression gains.

### 3 Methodology

#### 3.1 Preliminary

**Singular Value Decomposition.** Singular Value Decomposition [11] is a classical matrix factorization technique widely used for low-rank approximation. Given a matrix  $\mathbf{W} \in \mathbb{R}^{m \times n}$ , SVD factorizes it into three components:  $\mathbf{W} = \mathbf{U}\mathbf{\Sigma}\mathbf{V}^\top$ , where  $\mathbf{U} \in \mathbb{R}^{m \times m}$  and  $\mathbf{V} \in \mathbb{R}^{n \times n}$  are orthogonal matrices containing the left and right singular vectors, and  $\mathbf{\Sigma} \in \mathbb{R}^{m \times n}$  is a diagonal matrix with non-negative singular values. To obtain a low-rank approximation of a weight matrix  $\mathbf{W} \in \mathbb{R}^{m \times n}$ , we apply singular value decomposition (SVD) and retain only the top  $r$  singular values and their associated singular vectors. This results in an approximate factorization:

$$\mathbf{W} \approx \mathbf{L}\mathbf{R}, \quad \text{where } \mathbf{L} = \mathbf{U}_r\mathbf{\Sigma}_r^{1/2}, \quad \mathbf{R} = \mathbf{\Sigma}_r^{1/2}\mathbf{V}_r^\top. \quad (1)$$

Here,  $\mathbf{U}_r \in \mathbb{R}^{m \times r}$  and  $\mathbf{V}_r \in \mathbb{R}^{n \times r}$  are the top- $r$  singular vectors of  $\mathbf{W}$ , and  $\mathbf{\Sigma}_r \in \mathbb{R}^{r \times r}$  contains the corresponding singular values. This yields two smaller matrices,  $\mathbf{L}$  and  $\mathbf{R}$ , from the low-rank decomposition of  $\mathbf{W}$ . Given an input  $\mathbf{x} \in \mathbb{R}^{1 \times m}$ , we compute the intermediate representation  $\mathbf{z} = \mathbf{x}\mathbf{L}$  and store  $\mathbf{z} \in \mathbb{R}^{1 \times r}$  in the KV cache instead of the full output. During attention, the output is approximated by reconstructing  $\mathbf{x}\mathbf{W} \approx \mathbf{z}\mathbf{R}$ . This approach reduces the KV cache size with a compression ratio of  $r/n$ , while maintaining a close approximation of the original computation.

**Centered Kernel Alignment Similarity.** Centered Kernel Alignment (CKA) [15] is a widely used metric for quantifying the similarity between two sets of representations. Given two matrices  $\mathbf{X} \in \mathbb{R}^{n \times d_1}$  and  $\mathbf{Y} \in \mathbb{R}^{n \times d_2}$ , CKA is computed by first forming their Gram (kernel) matrices  $\mathbf{G}_\mathbf{X} = \mathbf{X}\mathbf{X}^\top$  and  $\mathbf{G}_\mathbf{Y} = \mathbf{Y}\mathbf{Y}^\top$ . These kernel matrices are then centered as follows:

$$\tilde{\mathbf{G}}_\mathbf{X} = \mathbf{H}\mathbf{G}_\mathbf{X}\mathbf{H}, \quad \tilde{\mathbf{G}}_\mathbf{Y} = \mathbf{H}\mathbf{G}_\mathbf{Y}\mathbf{H}, \quad (2)$$

where  $\mathbf{H} = \mathbf{I}_n - \frac{1}{n}\mathbf{1}_n\mathbf{1}_n^\top$  is the centering matrix. The final CKA similarity is defined as:

$$\text{CKA}(\mathbf{X}, \mathbf{Y}) = \frac{\text{HSIC}(\mathbf{X}, \mathbf{Y})}{\sqrt{\text{HSIC}(\mathbf{X}, \mathbf{X}) \cdot \text{HSIC}(\mathbf{Y}, \mathbf{Y})}}, \quad (3)$$

where  $\text{HSIC}(\mathbf{X}, \mathbf{Y}) = \text{Tr}(\tilde{\mathbf{G}}_{\mathbf{X}} \tilde{\mathbf{G}}_{\mathbf{Y}})$  denotes the Hilbert-Schmidt Independence Criterion (HSIC). CKA ranges from 0 to 1, with higher values indicating greater similarity between the two matrices.

### 3.2 Head-wise Similarity-aware Reordering

**Group-head Low-rank Decomposition.** Following the grouped decomposition strategy proposed in Palu [5], we organize multiple attention heads into groups prior to performing SVD. Given a Key projection matrix  $\mathbf{W} \in \mathbb{R}^{m \times n}$ , where  $n = h \cdot d_h$  corresponds to  $h$  attention heads each of hidden dimension  $d_h$ , we divide  $\mathbf{W}$  column-wise into  $h$  submatrices, each representing a single head. Then we group every  $s$  heads into one group, resulting in  $g = h/s$  groups in total. For each group  $j$ , we construct a concatenated projection matrix  $\mathbf{W}_{g_j} = [\mathbf{W}_{j,1}, \dots, \mathbf{W}_{j,s}]$ , where each  $\mathbf{W}_{j,k} \in \mathbb{R}^{m \times d_h}$  is the projection matrix of the  $k$ -th head in group  $j$ , and thus  $\mathbf{W}_{g_j} \in \mathbb{R}^{m \times (s \cdot d_h)}$ . Instead of applying SVD to the entire projection matrix at once, we apply low-rank approximation to the grouped matrix:  $\mathbf{W}_{g_j} \approx \mathbf{L}_{g_j} \mathbf{R}_{g_j}$ , where  $\mathbf{L}_{g_j} \in \mathbb{R}^{d \times r_g}$  and  $\mathbf{R}_{g_j} \in \mathbb{R}^{r_g \times (d_h \cdot s)}$ . During inference, the latent representation shared across all heads in the group is computed as:  $\mathbf{z}_{g_j} = \mathbf{x} \mathbf{L}_{g_j}$ , and the projected outputs for individual heads are reconstructed via:

$$[\mathbf{y}_{j,1}, \dots, \mathbf{y}_{j,s}] = \mathbf{z}_{g_j} \mathbf{R}_{g_j}. \quad (4)$$

This grouped strategy provides a good trade-off between reconstruction overhead and approximation fidelity, enabling efficient compression with minimal performance impact.

**CKA-based Head Similarity.** A key question in grouped SVD is how to assign attention heads into groups so as to minimize the reconstruction error. Empirically, we observe that grouping heads with similar left singular subspaces results in lower approximation error, as these heads tend to share more common representational components and thus benefit from joint compression. To quantify head similarity, we adopt centered kernel alignment (CKA) [15], a robust and widely used metric for comparing representation subspaces. Specifically, we compute the pairwise CKA similarity between all attention heads, yielding a symmetric similarity matrix  $\mathbf{S} \in \mathbb{R}^{h \times h}$ , where  $h$  is the total number of heads:

$$\mathbf{S}_{i,j} = \text{CKA}(\mathbf{H}_i, \mathbf{H}_j), \quad \forall i, j \in 1, \dots, h. \quad (5)$$

**Head Reordering.** Based on the similarity matrix  $\mathbf{S}$ , we perform head grouping by prioritizing pairs with high mutual similarity. Specifically, we adopt a greedy strategy that iteratively selects the head pair with the highest CKA similarity and assigns them to the same group, subject to a fixed group size constraint (e.g., 4 heads per group when  $h = 32$ ). Remaining unassigned heads are then added to existing groups with available capacity, ensuring that all heads are eventually grouped. This head reordering process encourages heads with similar representational structure to share SVD decompositions, effectively reducing approximation error during grouped compression. As shown in Figure 2, we visualize the CKA similarity matrices before and after head reordering. It can be observed that, after reordering, heads assigned to adjacent positions exhibit higher mutual similarity, indicating that similar heads are more effectively grouped together. By aligning structurally coherent heads within each group, we improve both the compactness and accuracy of the resulting low-rank representation. To ensure decoding equivalence, we apply an inverse reordering to restore the original head order after grouped computation (see Figure 3).

### 3.3 Offline Calibration and Matrix Fusion

**Offline Calibration.** For Value cache compression, we directly perform SVD on the full Value projection matrix  $\mathbf{W}_v \in \mathbb{R}^{m \times n}$ , resulting in the decomposed matrices:  $\mathbf{W}_v \approx \mathbf{L}_v \mathbf{R}_v$ , where  $\mathbf{L}_v \in \mathbb{R}^{m \times r}$  and  $\mathbf{R}_v \in \mathbb{R}^{r \times n}$  represent the compressed components of the original Value projection matrix

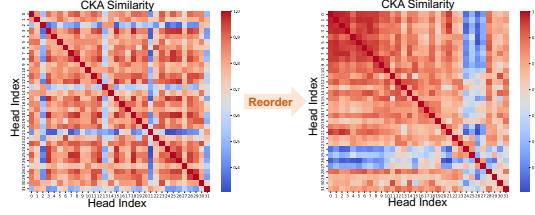


Figure 2: CKA similarity matrices before and after head reordering.

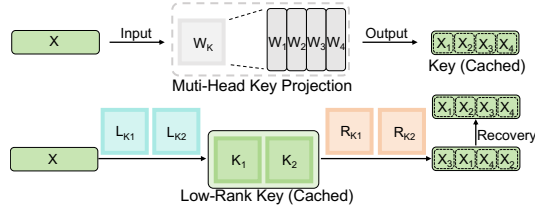


Figure 3: **Key decoding with HSR.** Similar heads are reordered and grouped before SVD, enabling more accurate reconstruction.

---

**Algorithm 1** Pseudocode of ReCalKV

---

```
1: Inputs: Model  $\mathcal{M}$ , Calibration Data  $\mathcal{X}$ , Target Compression Ratio  $\mathcal{TR}$ 
2: Output:  $\mathcal{M}'$ : Model equipped with compressed KV cache
3: procedure RECALKV( $\mathcal{M}, \mathcal{X}, \mathcal{TR}$ )
4:    $\mathcal{F} \leftarrow \text{CALCULATE\_FISHER\_INFO}(\mathcal{M}, \mathcal{X})$ 
5:    $R \leftarrow \text{ALLOCATE\_COMPRESSION\_RATIO}(\mathcal{M}, \mathcal{TR}, \mathcal{F})$ 
6:   for each Key projection layer  $\mathcal{W}_k$  in model  $\mathcal{M}$  do
7:      $\mathcal{CKA} \leftarrow \text{CALCULATE\_CKA\_SIMILARITY}(\mathcal{W}_k)$ 
8:      $\mathcal{W}'_k \leftarrow \text{HEAD\_REORDER}(\mathcal{W}_k, \mathcal{CKA})$ 
9:      $\mathbf{L}_k, \mathbf{R}_k \leftarrow \text{GROUP\_SVD}(\mathcal{W}'_k, R[\mathcal{W}_k])$ 
10:     $\mathcal{M}' \leftarrow \text{UPDATE\_LAYER}(\mathbf{L}_k, \mathbf{R}_k, \mathcal{W}_k, \mathcal{M})$ 
11:   end for
12:   for each Value projection layer  $\mathcal{W}_v$  in model  $\mathcal{M}$  do
13:      $\mathbf{L}_v, \mathbf{R}_v \leftarrow \text{SVD}(\mathcal{W}_v, R[\mathcal{W}_v])$ 
14:      $\mathbf{L}'_v, \mathbf{R}'_v \leftarrow \text{OFFLINE\_CALIBRATION}(\mathcal{W}_v, \mathbf{L}_v, \mathbf{R}_v, \mathcal{X})$ 
15:      $\mathcal{W}_o \leftarrow \text{MATRIX\_FUSION}(\mathbf{R}'_v, \mathcal{W}_o)$ 
16:      $\mathcal{M}' \leftarrow \text{UPDATE\_LAYER}(\mathbf{L}'_v, \mathcal{W}_v, \mathcal{M})$ 
17:      $\mathcal{M}' \leftarrow \text{UPDATE\_LAYER}(\mathcal{W}'_o, \mathcal{W}_o, \mathcal{M})$ 
18:   end for
19:   return  $\mathcal{M}'$ 
20: end procedure
```

---

$\mathbf{W}_v \in \mathbb{R}^{m \times n}$ . We then define the approximation error  $\mathcal{E}$  introduced by the SVD decomposition as:

$$\mathcal{E} = \|\mathbf{L}_v \mathbf{R}_v \mathbf{X} - \mathbf{W}_v \mathbf{X}\|_F^2, \quad (6)$$

where  $\mathbf{X}$  denotes the calibration dataset. Based on our analysis of Fisher Information, we observe that the Value projection matrix exhibits significantly higher Fisher Information compared to the Key projection matrix. This indicates that the Value projection matrix plays a more critical role in model performance. Therefore, we aim to minimize the approximation error  $\mathcal{E}$  introduced during the compression of the Value projection to preserve model accuracy as much as possible. Inspired by recent findings in adaptive decomposition methods such as AdaSVD [18], we observe that standard SVD decomposition does not always yield the lowest approximation error. To this end, we perform offline calibration of the decomposed matrices  $\mathbf{L}_v$  and  $\mathbf{R}_v$  using a small calibration dataset  $\mathbf{X}$ , aiming to further reduce the compression-induced approximation error. We first calibrate  $\mathbf{L}_v$  by setting the derivative of the approximation error  $\mathcal{E}$  with respect to  $\mathbf{L}_v$  to zero:

$$\frac{\partial \mathcal{E}}{\partial \mathbf{L}_v} = 0 \quad \Rightarrow \quad \mathbf{L}_v = \mathbf{W} \mathbf{X} \mathbf{X}^\top \mathbf{R}_v^\top (\mathbf{R}_v \mathbf{X} \mathbf{X}^\top \mathbf{R}_v)^{-1}. \quad (7)$$

Next, to improve the fidelity of the low-rank approximation, we calibrate the right factor  $\mathbf{R}_v$  by minimizing the approximation error. Specifically, we compute the gradient of the approximation error  $\mathcal{E}$  with respect to  $\mathbf{R}_v$  and set it to zero, allowing us to solve for a more accurate  $\mathbf{R}_v$  in closed form:

$$\frac{\partial \mathcal{E}}{\partial \mathbf{R}_v} = 0 \quad \Rightarrow \quad \mathbf{R}_v = ((\mathbf{L}_v)^\top \mathbf{L}_v)^{-1} (\mathbf{L}_v)^\top \mathbf{W}. \quad (8)$$

This yields an optimal closed-form solution for  $\mathbf{R}_v$ . Together, the calibrated  $\mathbf{L}_v$  and  $\mathbf{R}_v$  form a refined low-rank approximation of the original Value projection matrix, effectively reducing compression-induced error without incurring any additional inference-time computation. The derivation of the calibration objective and the resulting closed-form updates for both  $\mathbf{L}_v$  and  $\mathbf{R}_v$  are provided in the supplementary material, along with a detailed discussion of its implementation considerations.

**Matrix Fusion.** After performing SVD and offline calibration on the Value projection matrix, we further optimize the inference efficiency by eliminating unnecessary reconstruction steps. Specifically, instead of computing the full Value cache and then applying the output projection matrix  $\mathcal{W}_o$ , we fuse  $\mathbf{R}_v$  into  $\mathcal{W}_o$  to avoid runtime reconstruction. We start from the standard attention output:

$$\text{Output} = \text{Attention}(Q, K, V) \mathcal{W}_o = \text{Attention}(X \mathcal{W}_q, X \mathcal{W}_k, X \mathcal{W}_v) \mathcal{W}_o. \quad (9)$$

where  $X$  is the input sequence,  $\mathcal{W}_q$ ,  $\mathcal{W}_k$ , and  $\mathcal{W}_v$  are the projection matrices for query, key, and value respectively, and  $\mathcal{W}_o$  is the output projection matrix. For compressed Value cache, we store  $X' = X \mathbf{L}_v$  as the low-rank representation. With Value compression, the attention output becomes:

$$\text{Output} = \text{Attention}(X \mathcal{W}_q, X \mathcal{W}_k, X \mathbf{L}_v \mathbf{R}_v) \mathcal{W}_o. \quad (10)$$

We then define a fused output projection matrix  $\widetilde{W}_o = \mathbf{R}_v W_o$ , and compute the attention output as:

$$\text{Output} = \text{Attention}(XW_q, XW_k, X\mathbf{L}_v)\widetilde{W}_o. \quad (11)$$

This design eliminates the need to explicitly reconstruct  $X'\mathbf{R}_v$  during inference. By merging the computation into a single step, matrix fusion reduces both memory usage and computational overhead, streamlining the runtime execution path. Moreover, since the fused matrix  $\widetilde{W}_o$  can be precomputed entirely offline, it introduces no additional overhead to online inference, making this approach highly suitable for latency-sensitive applications and deployment on resource-constrained hardware.

### 3.4 ReCalKV Workflow

The overall pipeline of ReCalKV is outlined in Algorithm 1. Given a pre-trained model  $\mathcal{M}$ , calibration data  $\mathcal{X}$ , and a target compression ratio  $\mathcal{R}$ , ReCalKV applies differentiated compression strategies to Key and Value projection layers. We first compute layer-wise Fisher Information scores using the calibration data, following the strategy introduced in Palu [5], to estimate the relative importance of each layer and guide compression ratio allocation. Based on this, we allocate compression ratios to different layers accordingly. For Key projection layers, we first compute head-wise CKA similarity, then reorder the heads to group the most similar ones together, and finally apply grouped SVD for compression. For Value projection layers, we apply standard SVD followed by offline calibration to adjust the low-rank factors. Then we fuse the right factor of the decomposition with the output projection matrix  $W_o$  in the attention block. The modified matrices are then written back into the model. The final output is a modified model  $\mathcal{M}'$  that generates compressed KV caches.

## 4 Experiments

### 4.1 Experimental Settings

**Models.** We evaluate our method on a range of widely adopted LLMs, including multiple generations of the LLaMA family: LLaMA-7B [35], LLaMA-2-7B [36], and LLaMA-2-13B-Chat [36]. We also include instruction-tuned variants such as Mistral-7B-Instruct-v0.2 [14] and LongChat-7B-v1.5-32k [16] to assess performance under extended context settings. These models cover both base and chat/instruction-following variants, ensuring a comprehensive evaluation across different architectures and use cases. Notably, Mistral-7B-Instruct-v0.2 [14] adopt Grouped Query Attention (GQA) [1], while the others use standard Multi-Head Attention (MHA) [37].

**Datasets and Evaluation.** We assess the effectiveness of our method using both perplexity and task-specific accuracy. For language modeling evaluation, we report perplexity on WikiText2 [23], Penn Treebank (PTB)[28], and a subset of the C4 corpus[29]. To evaluate reasoning and generalization capabilities, we measure zero-shot accuracy on six QA benchmarks: ARC-c, ARC-e [6], Hellaswag [42], OBQA [24], PIQA [3], and Winogrande [31]. In addition, we adopt the LongBench benchmark [2] to evaluate long-context performance, conducting experiments on eight diverse tasks that comprehensively test the model’s ability to handle extended contexts.

**Baselines.** We compare our method with Palu [5], a recent low-rank compression approach for KV cache. Specifically, we adopt its G-LRD variant for evaluation. To ensure a fair comparison, we follow the same group-wise decomposition setting and fix the group size to 4 in all experiments.

**Implementation Details.** All experiments are conducted using PyTorch [27] and Huggingface Transformers [26] on a single NVIDIA A800 GPU with 80GB of memory. Following the setup in SVD-LLM [38], we apply a whitening transformation before performing SVD truncation. Specifically, we randomly select 256 samples from the WikiText-2 dataset as calibration data and use them both for whitening in the SVD step and for the offline calibration process in Value compression.

### 4.2 Main Results

**Perplexity Results.** We evaluate the language modeling capability of ReCalKV on three standard datasets: WikiText2 [23], PTB [28], and C4 [30], using perplexity as the evaluation metric. As shown in Table 1, ReCalKV achieves lower perplexity than Palu [5] on most compression ratios and model families. On LLaMA-2-7B [36], ReCalKV yields a perplexity of 5.83 on WikiText2 and 8.14 on C4 at 50% compression, compared to 6.02 and 8.72 from Palu, respectively. Similar trends are observed on LLaMA-7B [35] and Mistral-7B [14]. Notably, on PTB, ReCalKV significantly outperforms Palu under aggressive compression. For instance, at 70% compression, the perplexity of Palu rises sharply to 211.33 on LLaMA-7B and 172.23 on LongChat-7B, while ReCalKV keeps it much lower at 71.47

Table 1: Zero-shot performance comparison between **ReCalKV** and Palu [5] under 50% to 70% compression ratios. Evaluation on three language modeling datasets (measured by perplexity ( $\downarrow$ )) and six zero-shot QA datasets (measured by both individual and average accuracy ( $\uparrow$ )).

RATIO	METHOD	Wiki2 $\downarrow$	PTB $\downarrow$	C4 $\downarrow$	OBQA	Hella	PIQA	ARC-e	ARC-c	Wino	Average $\uparrow$
<b>LLaMA-7B [35]</b>											
0%	Original	5.68	41.15	7.34	44.40	76.18	78.67	75.25	44.80	70.01	64.89
50%	Palu [5]	6.27	48.39	8.85	41.6	73.46	76.71	72.35	40.53	68.75	62.23
	<b>ReCalKV</b>	<b>6.13</b>	<b>43.99</b>	<b>8.36</b>	<b>42.00</b>	<b>73.59</b>	<b>77.20</b>	<b>72.35</b>	<b>41.72</b>	<b>68.35</b>	<b>62.54</b>
60%	Palu [5]	7.08	91.45	10.98	36.80	68.80	73.94	67.63	38.14	63.61	58.15
	<b>ReCalKV</b>	<b>6.63</b>	<b>56.49</b>	<b>9.44</b>	<b>39.80</b>	<b>71.51</b>	<b>75.95</b>	<b>71.09</b>	<b>40.10</b>	<b>64.17</b>	<b>60.44</b>
70%	Palu [5]	8.42	211.33	14.46	34.60	61.06	71.00	61.53	33.70	59.51	53.57
	<b>ReCalKV</b>	<b>7.24</b>	<b>71.47</b>	<b>10.53</b>	<b>38.20</b>	<b>68.73</b>	<b>75.19</b>	<b>67.55</b>	<b>39.08</b>	<b>64.01</b>	<b>58.79</b>
<b>LLaMA-2-7B [36]</b>											
0%	Original	5.47	37.91	7.26	44.20	76.01	78.07	76.35	46.25	69.06	64.99
50%	Palu [5]	6.02	40.89	8.72	43.80	73.34	76.17	72.98	42.24	67.32	62.64
	<b>ReCalKV</b>	<b>5.83</b>	<b>39.51</b>	<b>8.14</b>	<b>45.00</b>	<b>74.39</b>	<b>76.39</b>	<b>74.71</b>	<b>43.52</b>	<b>67.80</b>	<b>63.64</b>
60%	Palu [5]	6.81	51.32	10.69	40.00	68.55	74.10	68.99	38.14	63.38	58.85
	<b>ReCalKV</b>	<b>6.21</b>	<b>65.73</b>	<b>8.95</b>	<b>41.40</b>	<b>72.36</b>	<b>76.17</b>	<b>72.73</b>	<b>41.13</b>	<b>68.03</b>	<b>61.97</b>
70%	Palu [5]	8.62	83.19	15.01	34.20	59.30	68.82	57.87	31.66	61.01	52.14
	<b>ReCalKV</b>	<b>6.75</b>	<b>75.78</b>	<b>10.05</b>	<b>39.80</b>	<b>69.59</b>	<b>74.48</b>	<b>70.37</b>	<b>39.42</b>	<b>65.75</b>	<b>59.90</b>
<b>Mistral-7B-Instruct-v0.2 [14]</b>											
0%	Original	5.94	32.46	9.72	46.80	83.68	80.41	81.31	55.63	74.35	70.36
50%	Palu [5]	6.33	37.38	10.79	44.60	80.89	79.33	79.21	54.27	73.40	68.62
	<b>ReCalKV</b>	<b>6.30</b>	<b>38.12</b>	<b>10.73</b>	<b>44.40</b>	<b>81.06</b>	<b>80.20</b>	<b>80.05</b>	<b>54.86</b>	<b>73.56</b>	<b>69.02</b>
60%	Palu [5]	7.07	49.45	12.93	42.80	75.30	77.26	74.07	50.00	70.72	65.03
	<b>ReCalKV</b>	<b>6.81</b>	<b>47.27</b>	<b>11.98</b>	<b>44.00</b>	<b>77.88</b>	<b>79.27</b>	<b>77.78</b>	<b>52.22</b>	<b>72.30</b>	<b>67.24</b>
70%	Palu [5]	8.71	77.51	16.78	38.60	66.48	75.24	66.96	42.49	66.54	59.39
	<b>ReCalKV</b>	<b>8.08</b>	<b>70.96</b>	<b>14.98</b>	<b>39.00</b>	<b>71.08</b>	<b>76.82</b>	<b>72.14</b>	<b>46.25</b>	<b>67.72</b>	<b>62.17</b>
<b>LongChat-7B-v1.5-32k [16]</b>											
0%	Original	7.61	89.04	10.52	41.40	71.28	76.12	71.84	41.38	68.19	61.70
50%	Palu [5]	8.11	120.11	12.08	38.20	68.30	72.52	67.93	38.40	64.96	58.39
	<b>ReCalKV</b>	<b>7.89</b>	<b>95.51</b>	<b>11.48</b>	<b>41.80</b>	<b>69.66</b>	<b>73.78</b>	<b>69.61</b>	<b>38.91</b>	<b>65.59</b>	<b>59.89</b>
60%	Palu [5]	9.15	168.94	14.42	37.80	64.76	69.70	60.14	34.64	61.09	54.68
	<b>ReCalKV</b>	<b>8.14</b>	<b>108.52</b>	<b>12.12</b>	<b>40.00</b>	<b>67.63</b>	<b>71.98</b>	<b>66.92</b>	<b>37.03</b>	<b>63.77</b>	<b>57.89</b>
70%	Palu [5]	11.95	172.23	20.87	32.20	54.94	64.74	50.00	28.67	55.56	47.69
	<b>ReCalKV</b>	<b>9.01</b>	<b>109.38</b>	<b>13.63</b>	<b>35.20</b>	<b>63.18</b>	<b>68.55</b>	<b>58.84</b>	<b>33.53</b>	<b>59.12</b>	<b>53.07</b>

and 109.38, respectively. These results demonstrate that ReCalKV maintains stronger language modeling ability under high compression. Even at 70% compression, perplexity degradation remains moderate, indicating better information preservation than existing low-rank methods.

**Zero-shot Accuracy Results.** In addition to perplexity, we evaluate ReCalKV on six zero-shot QA datasets, including OBQA [24], HellaSwag [43], PIQA [3], ARC-e [7], ARC-c [7], and Wino-grande [31]. Across all model families and compression levels, ReCalKV demonstrates strong resilience in accuracy. While both methods see a decline in performance as the compression ratio increases, Palu [5] exhibits a significantly steeper drop. For instance, at 70% compression on LLaMA-2-7B [36], Palu’s average accuracy drops to 52.14%, whereas ReCalKV retains 59.90%. Similar robustness is observed on Mistral-7B [14] and LongChat-7B [16], where ReCalKV consistently delivers higher or comparable average accuracy under the same compression levels. These results highlight ReCalKV’s strong capability to preserve task performance even under aggressive KV cache size reductions. Moreover, the method’s consistent stability across a wide range of tasks further underscores its practical utility for efficient long-context inference in real-world applications.

**Longbench Result.** We further evaluate ReCalKV on LongBench [2], a benchmark designed to test long-context understanding across diverse tasks. As shown in Table 2, ReCalKV achieves higher average accuracy than Palu [5] across nearly all model scales and compression ratios. The gap becomes especially pronounced at high compression levels (e.g., 70%), where Palu suffers significant

Table 2: Evaluation results on LongBench [2], covering accuracy across 8 tasks and the overall average, comparing **ReCalKV** and Palu [5] under 50%–70% KV cache compression ratios.

RATIO	METHOD	Qasper	QMSum	MultiNews	TREC	TriviaQA	SAMSum	LCC	RepoBench-P	Average↑
<b>LLaMA-2-7B [36]</b>										
0%	Original	9.58	21.22	3.51	66.00	87.72	41.66	66.68	59.80	44.52
50%	Palu [5]	8.40	18.93	1.31	61.50	84.56	38.40	50.90	46.80	38.85
	<b>ReCalKV</b>	<b>8.39</b>	<b>18.89</b>	<b>1.37</b>	<b>58.50</b>	<b>84.75</b>	<b>39.41</b>	<b>58.29</b>	<b>54.61</b>	<b>40.53</b>
60%	Palu [5]	5.10	16.51	2.13	55.50	59.84	33.13	29.62	33.56	29.42
	<b>ReCalKV</b>	<b>6.62</b>	<b>17.96</b>	<b>0.17</b>	<b>58.00</b>	<b>80.41</b>	<b>38.13</b>	<b>49.05</b>	<b>44.43</b>	<b>36.85</b>
70%	Palu [5]	4.54	9.99	1.40	39.00	16.98	19.18	1.75	7.52	13.26
	<b>ReCalKV</b>	<b>3.28</b>	<b>15.41</b>	<b>0.12</b>	<b>53.00</b>	<b>66.24</b>	<b>32.61</b>	<b>34.11</b>	<b>32.15</b>	<b>29.62</b>
<b>LLaMA-2-13B-Chat [36]</b>										
0%	Original	24.21	20.38	25.70	67.50	86.90	42.19	50.06	50.55	45.94
50%	Palu [5]	24.65	21.03	24.21	67.00	83.75	40.73	37.81	38.35	42.19
	<b>ReCalKV</b>	<b>19.30</b>	<b>20.47</b>	<b>24.32</b>	<b>68.00</b>	<b>83.82</b>	<b>40.96</b>	<b>29.72</b>	<b>36.41</b>	<b>40.38</b>
60%	Palu [5]	17.65	20.27	21.76	65.00	79.25	36.49	34.04	29.91	38.05
	<b>ReCalKV</b>	<b>17.16</b>	<b>20.12</b>	<b>24.30</b>	<b>65.00</b>	<b>80.77</b>	<b>39.22</b>	<b>39.33</b>	<b>37.46</b>	<b>40.42</b>
70%	Palu [5]	17.99	19.10	17.11	59.5	62.44	29.45	8.73	18.09	29.05
	<b>ReCalKV</b>	<b>16.47</b>	<b>20.22</b>	<b>22.18</b>	<b>62.50</b>	<b>76.87</b>	<b>35.50</b>	<b>30.79</b>	<b>26.51</b>	<b>36.38</b>
<b>Mistral-7B-Instruct-v0.2 [14]</b>										
0%	Original	32.51	24.29	26.96	71.00	86.23	42.95	55.89	54.12	49.24
50%	Palu [5]	31.16	23.76	25.82	69.50	83.12	39.15	42.01	45.18	44.96
	<b>ReCalKV</b>	<b>31.71</b>	<b>23.35</b>	<b>26.43</b>	<b>70.00</b>	<b>82.51</b>	<b>39.22</b>	<b>46.12</b>	<b>45.21</b>	<b>45.57</b>
60%	Palu [5]	21.21	23.73	24.75	68.00	76.59	36.14	26.24	30.48	38.39
	<b>ReCalKV</b>	<b>24.98</b>	<b>24.26</b>	<b>25.32</b>	<b>71.00</b>	<b>75.53</b>	<b>37.42</b>	<b>34.28</b>	<b>36.79</b>	<b>41.19</b>
70%	Palu [5]	6.59	21.35	17.84	61.00	44.73	28.06	15.05	21.87	27.06
	<b>ReCalKV</b>	<b>9.13</b>	<b>23.01</b>	<b>20.85</b>	<b>65.00</b>	<b>51.44</b>	<b>31.37</b>	<b>15.13</b>	<b>22.66</b>	<b>29.82</b>
<b>LongChat-7B-v1.5-32k [16]</b>										
0%	Original	29.32	22.81	26.61	66.50	83.99	40.83	53.02	56.94	47.50
50%	Palu [5]	21.77	21.93	23.65	64.00	76.68	39.46	38.49	43.57	41.19
	<b>ReCalKV</b>	<b>25.15</b>	<b>22.08</b>	<b>23.38</b>	<b>63.00</b>	<b>79.75</b>	<b>40.72</b>	<b>50.54</b>	<b>50.52</b>	<b>44.39</b>
60%	Palu [5]	13.12	21.97	19.07	55.50	66.14	34.68	42.01	16.55	33.63
	<b>ReCalKV</b>	<b>20.99</b>	<b>21.13</b>	<b>22.68</b>	<b>59.00</b>	<b>76.12</b>	<b>38.78</b>	<b>40.45</b>	<b>40.91</b>	<b>40.01</b>
70%	Palu [5]	6.27	19.05	14.47	37.50	36.75	21.95	2.09	5.45	17.94
	<b>ReCalKV</b>	<b>17.50</b>	<b>20.70</b>	<b>18.94</b>	<b>44.00</b>	<b>67.29</b>	<b>33.86</b>	<b>10.48</b>	<b>15.23</b>	<b>28.50</b>

degradation while ReCalKV maintains competitive performance. This demonstrates ReCalKV’s robustness and suitability for long-sequence inference under memory constraints.

### 4.3 Ablation study

To analyze the individual contributions of each component in ReCalKV, we conduct ablation studies on LLaMA-2-7B [36] under a fixed 80% compression ratio. Table 3 reports perplexity on WikiText-2 [23], PTB [28], and C4 [30], as well as accuracy on two downstream evaluation suites: the average accuracy over six zero-shot QA datasets (**zero-shot Avg. Acc**) and the average accuracy across eight tasks from the LongBench benchmark [2] (**LongBench Avg. Acc**).

**Ablation on Head-wise Similarity-aware Reordering (HSR).** By comparing the first and second rows in Table 3, we observe that enabling HSR alone (without offline calibration) significantly improves performance. For example, perplexity on WikiText-2 drops from 9.34 to 9.01, and LongBench accuracy increases from 9.01% to 12.44%. These results suggest that the reordering strategy in HSR effectively groups similar attention heads together before applying SVD, which reduces approximation error during low-rank decomposition and leads to improved model performance.

**Ablation on Offline Calibration.** Comparing the first and third rows, we assess the effect of offline calibration alone. Perplexity on WikiText-2 improves from 9.34 to 8.91, while LongBench accuracy rises to 13.09%. This confirms that calibrating the SVD decomposition of the Value projection matrix using a small held-out dataset effectively improves the quality of approximation, thereby enhancing model performance and robustness across tasks.

### 4.4 Integrate with KV Cache Quantization

Since ReCalKV reduces the hidden dimension of the KV cache, it is inherently orthogonal and thus complementary to KV cache quantization techniques, which compress along the bitwidth axis.



Table 3: Ablation studies on LLaMA-2-7B are conducted at a fixed 80% compression ratio. Perplexity is reported on WikiText-2, PTB, and C4, with our results in **bold**.

HSR Strategy	Offline Calibration	WikiText2↓	PTB↓	C4↓	zero-shot Avg. Acc↑	LongBench Avg. Acc↑
×	×	9.34	92.52	14.58	49.01	9.01
✓	×	9.01	87.58	14.16	52.33	12.44
×	✓	8.91	81.96	14.08	52.98	13.09
✓	✓	<b>8.48</b>	<b>79.04</b>	<b>13.29</b>	<b>54.55</b>	<b>15.40</b>

This orthogonality enables seamless integration of the two methods for further compression. To assess their compatibility, we conduct experiments under various compression settings by combining ReCalKV with different quantization bitwidths (e.g., 4-bit and 3-bit), and varying the average rank to simulate different compression ratios. In our implementation, we adopt a per-token quantization scheme, allowing finer-grained control over dynamic range across sequence positions. Additionally, following Palu [5], we apply a randomized Hadamard transform prior to quantization to enhance robustness and reduce activation variance. Experimental results, as shown in Table 4, demonstrate that ReCalKV consistently outperforms Palu under the same compression ratio and bitwidth settings. For example, at a 60% compression ratio with 4-bit quantization, ReCalKV achieves a perplexity of 6.24 on WikiText-2, outperforming Palu’s 6.84. At 70% compression with 3-bit quantization, ReCalKV improves perplexity on C4 from 15.75 (Palu) to 10.41. These results confirm the effectiveness of combining ReCalKV with quantization for efficient KV cache compression.

Table 4: ReCalKV with KV cache quantization.

RATIO	METHOD	BIT	WikiText-2↓	C4↓
0%	Original	16	5.47	7.26
50%	Palu [5]	4	6.04	8.75
	Palu [5]	3	6.15	8.92
	ReCalKV	4	<b>5.86</b>	<b>8.18</b>
	ReCalKV	3	<b>5.96</b>	<b>8.34</b>
60%	Palu [5]	4	6.84	10.77
	Palu [5]	3	7.01	11.06
	ReCalKV	4	<b>6.24</b>	<b>9.01</b>
	ReCalKV	3	<b>6.39</b>	<b>9.21</b>
70%	Palu [5]	4	8.71	15.17
	Palu [5]	3	9.04	15.75
	ReCalKV	4	<b>6.79</b>	<b>10.11</b>
	ReCalKV	3	<b>7.01</b>	<b>10.41</b>

## 5 Discussion

**Limitations.** While ReCalKV demonstrates high compression ratio with minimal accuracy drop, there remain several limitations to be addressed. First, despite our efforts to preserve performance, the compressed models still exhibit a certain degree of degradation in metrics such as perplexity and accuracy compared to the full KV cache baseline. This indicates that our method, like most lossy compression approaches, cannot fully maintain the original model behavior under high compression ratios. Second, ReCalKV currently focuses on hidden dimension reduction and does not incorporate token eviction strategies, which aim to reduce the KV cache length dimension. As these two directions are complementary, future work could explore the integration of ReCalKV with token eviction methods to further improve memory efficiency while maintaining performance.

**Social Impacts.** ReCalKV offers a practical and effective solution for compressing the KV cache in LLMs, significantly reducing memory consumption during long-context inference. This reduction in computational and memory requirements can lower both the deployment cost and energy consumption, thereby enabling wider access to LLMs in resource-constrained environments such as edge devices and developing regions. Although compression may lead to slight performance degradation, the trade-off is often acceptable in exchange for improved efficiency and scalability. By facilitating more sustainable and accessible AI deployment, ReCalKV contributes to the broader goal of inclusive and environmentally responsible AI development.

## 6 Conclusion

In this work, we propose ReCalKV, a post-training KV cache compression framework tailored for efficient long-context reasoning in LLMs. By exploiting the distinct characteristics of Keys and Values in the attention mechanism, ReCalKV applies Head-wise Similarity-aware Reordering (HSR) and grouped SVD to compress Keys, while employing Offline Calibration and Matrix Fusion (OCMF) to compress Values. This design reduces hidden dimensions with minimal additional computation and preserves model performance under high compression ratios. Experimental results demonstrate that ReCalKV consistently outperforms existing low-rank compression methods, offering a practical and effective solution for memory-efficient LLM serving. Moreover, it can be combined with quantization to achieve higher compression with minimal performance loss. We believe this work provides a promising direction for scalable, long-context LLM deployment.

## References

- [1] Joshua Ainslie, James Lee-Thorp, Michiel de Jong, Yury Zemlyanskiy, Federico Lebrón, and Sumit Sanghai. Gqa: Training generalized multi-query transformer models from multi-head checkpoints. *arXiv preprint arXiv:2305.13245*, 2023.
- [2] Yushi Bai, Xin Lv, Jiajie Zhang, Hongchang Lyu, Jiankai Tang, Zhidian Huang, Zhengxiao Du, Xiao Liu, Aohan Zeng, Lei Hou, Yuxiao Dong, Jie Tang, and Juanzi Li. Longbench: A bilingual, multitask benchmark for long context understanding. *arXiv preprint arXiv:2308.14508*, 2023.
- [3] Yonatan Bisk, Rowan Zellers, Jianfeng Gao, Yejin Choi, et al. Piqa: Reasoning about physical commonsense in natural language. In *AAAI*, 2020.
- [4] Chi-Chih Chang, Chien-Yu Lin, Yash Akhauri, Wei-Cheng Lin, Kai-Chiang Wu, Luis Ceze, and Mohamed S Abdelfattah. xkv: Cross-layer svd for kv-cache compression. *arXiv preprint arXiv:2503.18893*, 2025.
- [5] Chi-Chih Chang, Wei-Cheng Lin, Chien-Yu Lin, Chong-Yan Chen, Yu-Fang Hu, Pei-Shuo Wang, Ning-Chi Huang, Luis Ceze, and Kai-Chiang Wu. Palu: Compressing kv-cache with low-rank projection. *arXiv preprint arXiv:2407.21118*, 2024.
- [6] Peter Clark, Isaac Cowhey, Oren Etzioni, Tushar Khot, Ashish Sabharwal, Carissa Schoenick, and Oyvind Tafjord. Think you have solved question answering? try arc, the ai2 reasoning challenge. *arXiv preprint arXiv:1803.05457*, 2018.
- [7] Peter Clark, Isaac Cowhey, Oren Etzioni, Tushar Khot, Ashish Sabharwal, Carissa Schoenick, and Oyvind Tafjord. Think you have solved question answering? try arc, the ai2 reasoning challenge. *arXiv:1803.05457v1*, 2018.
- [8] Harry Dong, Xinyu Yang, Zhenyu Zhang, Zhangyang Wang, Yuejie Chi, and Beidi Chen. Get more with less: Synthesizing recurrence with kv cache compression for efficient llm inference. *arXiv preprint arXiv:2402.09398*, 2024.
- [9] Abhimanyu Dubey, Abhinav Jauhri, Abhinav Pandey, Abhishek Kadian, Ahmad Al-Dahle, Aiesha Letman, Akhil Mathur, Alan Schelten, Amy Yang, Angela Fan, et al. The llama 3 herd of models. *arXiv preprint arXiv:2407.21783*, 2024.
- [10] Yu Fu, Zefan Cai, Abedelkadir Asi, Wayne Xiong, Yue Dong, and Wen Xiao. Not all heads matter: A head-level kv cache compression method with integrated retrieval and reasoning. *arXiv preprint arXiv:2410.19258*, 2024.
- [11] Gene H Golub, Alan Hoffman, and Gilbert W Stewart. A generalization of the eckart-young-mirsky matrix approximation theorem. *Linear Algebra and its applications*, 1987.
- [12] Coleman Hooper, Sehoon Kim, Hiva Mohammadzadeh, Michael W Mahoney, Yakun Sophia Shao, Kurt Keutzer, and Amir Gholami. Kvquant: Towards 10 million context length llm inference with kv cache quantization. *arXiv preprint arXiv:2401.18079*, 2024.
- [13] Yen-Chang Hsu, Ting Hua, Sungen Chang, Qian Lou, Yilin Shen, and Hongxia Jin. Language model compression with weighted low-rank factorization. In *ICLR*, 2022.
- [14] Albert Q. Jiang, Alexandre Sablayrolles, Arthur Mensch, Chris Bamford, Devendra Singh Chaplot, Diego de las Casas, Florian Bressand, Gianna Lengyel, Guillaume Lample, Lucile Saulnier, L  lio Renard Lavaud, Marie-Anne Lachaux, Pierre Stock, Teven Le Scao, Thibaut Lavril, Thomas Wang, Timoth  e Lacroix, and William El Sayed. Mistral 7b. *arXiv:2310.06825*, 2023.
- [15] Simon Kornblith, Mohammad Norouzi, Honglak Lee, and Geoffrey Hinton. Similarity of neural network representations revisited. In *NeurIPS*, 2019.
- [16] Dacheng Li, Rulin Shao, Anze Xie, Ying Sheng, Lianmin Zheng, Joseph Gonzalez, Ion Stoica, Xuezhe Ma, and Hao Zhang. How long can context length of open-source llms truly promise? In *NeurIPS Workshop*, 2023.
- [17] Yuhong Li, Yingbing Huang, Bowen Yang, Bharat Venkitesh, Acyr Locatelli, Hanchen Ye, Tianle Cai, Patrick Lewis, and Deming Chen. Snapkv: Llm knows what you are looking for before generation. In *NeurIPS*, 2024.
- [18] Zhiteng Li, Mingyuan Xia, Jingyuan Zhang, Zheng Hui, Linghe Kong, Yulun Zhang, and Xiaokang Yang. Adasvd: Adaptive singular value decomposition for large language models. *arXiv preprint arXiv:2502.01403*, 2025.

- [19] Bokai Lin, Zihao Zeng, Zipeng Xiao, Siqi Kou, Tianqi Hou, Xiaofeng Gao, Hao Zhang, and Zhijie Deng. Matryoshkakv: Adaptive kv compression via trainable orthogonal projection. *arXiv preprint arXiv:2410.14731*, 2024.
- [20] Aixin Liu, Bei Feng, Bin Wang, Bingxuan Wang, Bo Liu, Chenggang Zhao, Chengqi Deng, Chong Ruan, Damai Dai, Daya Guo, et al. Deepseek-v2: A strong, economical, and efficient mixture-of-experts language model. *arXiv preprint arXiv:2405.04434*, 2024.
- [21] Akide Liu, Jing Liu, Zizheng Pan, Yefei He, Reza Haffari, and Bohan Zhuang. Minicache: Kv cache compression in depth dimension for large language models. In *NeurIPS*, 2024.
- [22] Zirui Liu, Jiayi Yuan, Hongye Jin, Shaochen Zhong, Zhaozhuo Xu, Vladimir Braverman, Beidi Chen, and Xia Hu. Kivi: A tuning-free asymmetric 2bit quantization for kv cache. *arXiv preprint arXiv:2402.02750*, 2024.
- [23] Stephen Merity, Caiming Xiong, James Bradbury, and Richard Socher. Pointer sentinel mixture models. In *ICLR*, 2017.
- [24] Todor Mihaylov, Peter Clark, Tushar Khot, and Ashish Sabharwal. Can a suit of armor conduct electricity? a new dataset for open book question answering. *arXiv preprint arXiv:1809.02789*, 2018.
- [25] Matan Ben Noach and Yoav Goldberg. Compressing pre-trained language models by matrix decomposition. In *AACL/IJCNLP*, 2020.
- [26] A Paszke, S Gross, F Massa, A Lerer, JP Bradbury, G Chanan, T Killeen, Z Lin, N Gimelshein, L Antiga, et al. An imperative style, high-performance deep learning library. In *NeurIPS*, 2019.
- [27] Adam Paszke, Sam Gross, Francisco Massa, Adam Lerer, James Bradbury, Gregory Chanan, Trevor Killeen, Zeming Lin, Natalia Gimelshein, Luca Antiga, et al. Pytorch: An imperative style, high-performance deep learning library. In *NeurIPS*, 2019.
- [28] Tobias Plotz and Stefan Roth. Benchmarking denoising algorithms with real photographs. In *CVPR*, 2017.
- [29] Colin Raffel, Noam Shazeer, Adam Roberts, Katherine Lee, Sharan Narang, Michael Matena, Yanqi Zhou, Wei Li, and Peter J Liu. Exploring the limits of transfer learning with a unified text-to-text transformer. *JMLR*, 2020.
- [30] Colin Raffel, Noam Shazeer, Adam Roberts, Katherine Lee, Sharan Narang, Michael Matena, Yanqi Zhou, Wei Li, and Peter J Liu. Exploring the limits of transfer learning with a unified text-to-text transformer. *JMLR*, 2020.
- [31] Keisuke Sakaguchi, Ronan Le Bras, Chandra Bhagavatula, and Yejin Choi. Winogrande: An adversarial winograd schema challenge at scale. In *AAAI*, 2020.
- [32] Utkarsh Saxena, Gobinda Saha, Sakshi Choudhary, and Kaushik Roy. Eigen attention: Attention in low-rank space for kv cache compression. *arXiv preprint arXiv:2408.05646*, 2024.
- [33] Noam Shazeer. Fast transformer decoding: One write-head is all you need. *arXiv preprint arXiv:1911.02150*, 2019.
- [34] Jianlin Su, Murtadha Ahmed, Yu Lu, Shengfeng Pan, Wen Bo, and Yunfeng Liu. Roformer: Enhanced transformer with rotary position embedding. *Neurocomputing*, 568:127063, 2024.
- [35] Hugo Touvron, Thibaut Lavril, Gautier Izacard, Xavier Martinet, Marie-Anne Lachaux, Timothée Lacroix, Baptiste Rozière, Naman Goyal, Eric Hambro, Faisal Azhar, et al. Llama: Open and efficient foundation language models. *arXiv preprint arXiv:2302.13971*, 2023.
- [36] Hugo Touvron, Louis Martin, Kevin Stone, Peter Albert, Amjad Almahairi, Yasmine Babaei, Nikolay Bashlykov, Soumya Batra, Prajjwal Bhargava, and Others. Llama 2: Open foundation and fine-tuned chat models. *arXiv preprint arXiv:2307.09288*, 2023.
- [37] A Vaswani. Attention is all you need. In *NeurIPS*, 2017.
- [38] Xin Wang, Yu Zheng, Zhongwei Wan, and Mi Zhang. Svd-llm: Truncation-aware singular value decomposition for large language model compression. *arXiv preprint arXiv:2403.07378*, 2024.
- [39] Guangxuan Xiao, Yuandong Tian, Beidi Chen, Song Han, and Mike Lewis. Efficient streaming language models with attention sinks. In *ICLR*, 2023.

- [40] Zhihang Yuan, Yuzhang Shang, Yue Song, Qiang Wu, Yan Yan, and Guangyu Sun. Asvd: Activation-aware singular value decomposition for compressing large language models. *arXiv preprint arXiv:2312.05821*, 2023.
- [41] Yuxuan Yue, Zhihang Yuan, Haojie Duanmu, Sifan Zhou, Jianlong Wu, and Liqiang Nie. Wkvquant: Quantizing weight and key/value cache for large language models gains more. *arXiv preprint arXiv:2402.12065*, 2024.
- [42] Rowan Zellers, Ari Holtzman, Yonatan Bisk, Ali Farhadi, and Yejin Choi. Hellaswag: Can a machine really finish your sentence? In *ACL*, 2019.
- [43] Rowan Zellers, Ari Holtzman, Yonatan Bisk, Ali Farhadi, and Yejin Choi. Hellaswag: Can a machine really finish your sentence? *arXiv preprint arXiv:1905.07830*, 2019.
- [44] Rongzhi Zhang, Kuang Wang, Liyuan Liu, Shuohang Wang, Hao Cheng, Chao Zhang, and Yelong Shen. Lorc: Low-rank compression for llms kv cache with a progressive compression strategy. *arXiv preprint arXiv:2410.03111*, 2024.
- [45] Zhenyu Zhang, Ying Sheng, Tianyi Zhou, Tianlong Chen, Lianmin Zheng, Ruisi Cai, Zhao Song, Yuandong Tian, Christopher Ré, Clark Barrett, et al. H2o: Heavy-hitter oracle for efficient generative inference of large language models. In *NeurIPS*, 2023.
- [46] Yilong Zhao, Chien-Yu Lin, Kan Zhu, Zihao Ye, Lequn Chen, Size Zhenga, Luis Ceze, Arvind Krishnamurthy, Tianqi Chen, and Baris Kasikci. Atom: Low-bit quantization for efficient and accurate llm serving. *arXiv preprint arXiv:2310.19102*, 2023.